Cytotoxicity and apoptotic-inducing effect of 1-(1-tosyl-1H-indol-3yl)propan-1-one against lung cancer cells

Joao Henrique Oliveira Bonifacio
Health Science Graduate Program, Federal University of Sergipe
Mariana Nobre Farias Franca
Health Science Graduate Program, Federal University of Sergipe
Marcos Vinicius Barbosa Melo
Physiological Sciences Graduate Program, Federal University of Sergipe
Jileno Ferreira Santos
Physiological Sciences Graduate Program, Federal University of Sergipe
Cristiane Almeida Santos Oliveira
Physiological Sciences Graduate Program, Federal University of Sergipe
Ricardo Guimaraes Amaral
Medicine Department, Federal University of Sergipe
Sócrates Cabral de Holanda Cavalcanti
Pharmacy Department, Federal University of Sergipe
Cristiane Bani Correa
crisbani@gmail.com

Health Science Graduate Program, Federal University of Sergipe

Research Article

Keywords: Antineoplastics, Neoplasms, Indole, Flow cytometry

Posted Date: September 2nd, 2024

DOI: https://doi.org/10.21203/rs.3.rs-4857063/v1

Additional Declarations: No competing interests reported.

Abstract

Background

Lung cancer is the most prevalent and deadly cancer in the world. In the search for new antineoplastic drugs, research into derivatives of natural products revealed the constant evolution of science to provide treatments with fewer adverse effects. Indole is a natural compound found in plants and microorganisms with proven antitumor activity. Modifications to its structure can potentiate its cytotoxic effect on tumor cells. Thus, the aim of this study was to evaluate the cytotoxic potential of the synthetic indole derivative 1-(1-tosyl-1*H*-indol-3-yl)propan-1-one in tumor cell lines.

Methods

Sulforhodamine B (SRB) was used to evaluate the cytotoxic effect of compound 1-(1-tosyl-1*H*-indol-3-yl)propan-1-one against lung cancer (A549), breast cancer (MCF7) and prostate cancer (PC-3) cell lines. Furthermore, the hemolysis assay was carried out on human erythrocytes. The clonogenic and wound healing assays were used to analyze the reduction in colony formation and the migratory capacity of the A549 cell line, respectively. DAPI and Phalloidin/FITC were used to observe morphological changes. Death by apoptosis and necrosis were assessed by flow cytometer.

Results

The highest inhibitory effect was observed in the A549 cell line, with an IC_{50} of 2.6 μM. The A549 cell line was further selected for additional biological tests, considering the IC_{50} and the epidemiological relevance of this cancer. No hemolytic activity was observed in human erythrocytes after exposure to 1-(1-tosyl-1*H*-indol-3-yl)propan-1-one. In the colony formation test, clone inhibition was observed in the A549 cell line at a concentration of 5.2 μM. In the migration analysis, we observed that the compound inhibited wound closure in the A549 cells at the highest concentrations after 48 h of treatment. In addition, morphological changes characteristic of apoptosis, such as cytoplasmic reduction and changes in the disposition of actin filaments, were observed in the A549 cell line by staining with DAPI and phalloidin/FITC dyes. These results corroborate the flow cytometry results, which showed that the treatment induced apoptosis in the A549 cells.

Conclusions

Our results showed that the compound 1-(1-tosyl-1*H*-indol-3-yl)propan-1-one inhibited cell growth, migration and colony formation and promote cell death via apoptosis in A549 cell line.

1 BACKGROUND

Lung cancer is classified into two major groups: small cell carcinomas and non-small cell carcinomas. Among non-small cell carcinomas, adenocarcinomas are of utmost importance to the medical community because they are the most common histological subtype of lung cancer and one of the most fatal tumors, with an overall survival of 5 years. (Pêgo-Fernandes et al., 2021; Hutchinson et al., 2019; Denisenko et al., 2018). According to the Global Cancer Observatory (GLOBOCAN), 21 million new cases and 10 million deaths from cancer are expected to occur worldwide by 2025, with the tracheal, bronchial and lung cancers being one of the most prevalent, with 2,661,254 cases.

Surgery, chemotherapy and radiotherapy are considered the basis of treatment for lung cancer (Guerra et al., 2019). Although the effectiveness of these treatments has been proven, the adverse effects associated with them directly affect patient quality of life. In chemotherapy, the lack of selectivity in drug administration for cancer treatment often results in the unintended destruction of non-tumor cells (Silava et al., 2022; Faroni et al., 2022; Carvalho 2002; INCA, 2022).

In view of the incidence and prevalence rates of lung cancer, as well as the heterogeneity of the disease and traditional antineoplastic drug chemoresistance, there is a clear need to search for new compounds that are specific to tumor cells and have low toxicity to nontumor cells, providing an effective treatment with fewer adverse effects (de Franca et al., 2021; Yeldag et al., 2018).

Natural products are an important source of biologically active molecules, and approximately 40% of the drugs approved for commercialization are of natural origin. Specifically, in cancer, 64.9% of existing antineoplastic drugs are derived from natural sources (Newman & cragg, 2020). Research into the use of synthetic natural product derivatives for the treatment of cancer is growing (Asma et al., 2022). These synthetic derivatives with proven biological activity can present enhanced kinetic profiles, compared to their molecules of origin, with the possibility of modifying, for example, the absorption profile, as well as increasing cytotoxicity to tumor cells and decreasing toxic effects on nontumor cells, and increasing their selectivity and potency (Ottoni et al., 2013).

Among natural products, indole is an aromatic heterocyclic organic compound that has an indole core and is highly useful for the synthesis of new compounds due to its versatility. Certainly, the indole nucleus is the basis of several molecular structures of drugs already approved for commercialization, such as sumatriptan, tadalafil, fluvastatin and mitomycin (Dadashpour et al., 2018; Singh et al., 2018). In addition, indole has a proven cytotoxic effect on glioma, lung adenocarcinoma, melanoma (Andrade et al., 2024; Ramirez et al., 2020; Sabol et al., 2000) and breast cancer (Kelly et al., 2016) tumor cells lines, showing its importance in the search for potential new antineoplastic drugs.

Our group recently evaluated the activity of synthetic indole derivatives, wich demonstrated the anti-proliferative and anti-migratory activity of Phenyl(1-tosyl-1H-indol-3-yl)methanone against glioma cells (Andrade et al., 2024). These synthetic indole derivatives exhibited higher lung cancer and melanoma cells activity compared to indole. In view of the cytotoxic potential of indole and its synthetic derivatives, and the versatility of this compound, the aim of this study was to evaluate the cytotoxic potential of the synthetic indol derivative 1-(1-tosyl-1*H*-indol-3-yl)propan-1-one against lung cancer cell line A549.

2 METHODS

2.1 Chemicals

The experiments used Dulbeccos's Modified Eagle Medium (DMEM), Trypsin, EDTA, DMSO, DAPI, SRB, Triton X 100 and Phalloidin-FITC from Sigma Aldrich (Saint Louis, MO, USA); SFB, antibiotics (penicillin 10000 U/mL; streptomycin 10000 mg/mL), Doxorubicin hydrochloride (Libbis, Embu das Artes, São Paulo, Brazil); Trichloroacetic acid (Neon, São Paulo, Brazil); Acetic acid (Synth, Diadema, São Paulo, Brazil); TRIS-base (Inlab Confiança, Brazil); Trypan blue (Sigma); Compound NM-01-24-19.

2.2 Chemistry

2.2.1 General

Melting point was obtained using a Logen Scientific melting point apparatus and temperature values were uncorrected. NMR data were recorded in $CDCl_3$ at 293 K on an Agilent/Varian 500 MHz DD2, observing ^{1}H and ^{13}C at 500 and 125 MHz, respectively. All ^{1}H and ^{13}C NMR chemical shifts (δ) are given in ppm related to the TMS signal at 0.00 ppm as internal reference. Coupling constants (J) are reported in hertz (Hz). The abbreviations used are s (singlet), d (doublet), t (triplet), q (quartet), and m (multiplet). FT-IR spectrum was recorded with a PerkinElmer Spectrum BX FT-IR system. Mass spectrum was recorded with a Bruker micrOTOF II - ESI-TOF mass spectrometer operating in positive mode. Reactions were monitored by thin-layer chromatography (TLC) using suitable mobile phase eluents, and visualization of the TLC plate was accomplished with UV light at 256 nm and suitable TLC visualization reagents. Details of the physicochemical properties of the synthesized compounds are described below. General chemicals were obtained from Sigma-Aldrich Chemical Co. (St. Louis, MO, USA).

2.3 Synthesis

2.3.1 Synthesis of *N*-tosylindole (1)

N-tosylindole was synthesized according to the procedure reported by Andrade et al., (2024).

2.3.2 Synthesis of 1-(1-tosyl-1*H*-indol-3-yl)propan-1-one (2)

To a stirred mixture of $AlCl_3$ (3 mmol) and propionyl chloride (1.5 mmol) in dry dichloromethane (DCM) (5 mL) at room temperature, a solution of *N*-tosylindole (0.271 g, 1 mmol) in dry DCM (2 mL) was added dropwise. The mixture was then stirred at room temperature for 1.5 h, and the reaction process was checked by TLC analysis. Next, water (10 mL) was added to the mixture, which was extracted with $CHCl_3$ (30 mL × 3). The combined organic phase was washed with saturated aqueous $NaHCO_3$ (30 mL × 2) and brine (30 mL), dried over anhydrous Na_2SO_4, concentrated under vacuum, and purified by silica gel column chromatography (60–100% $CHCl_3$: Hex) to afford 1-(1-tosyl-1*H*-indol-3-yl)propan-1-one in 74% yield. White crystals. (74.3%), mp 112–115°C. IR (KBr, cm-1) 1662. ^{1}H NMR (500 MHz, $CDCl_3$) δ 8.33–8.37 (m, 1H), 8.24 (s, 1H), 7.94 (d, J = 7.34 Hz, 1H), 7.84 (d, J = 8.31 Hz, 2H), 7.32–7.40 (m, 2H), 7.28 (d, J = 8.80 Hz, 2H),

2.95 (q, *J* = 7.34 Hz, 2H), 2.37 (s, 3H), 1.26 (t, *J* = 7.34 Hz, 3H). ^{13}C NMR (125 MHz, $CDCl_3$) δ 196.8, 145.9, 134.9, 134.5, 131.5, 130.2, 127.7, 127.1, 125.7, 124.8, 123.1, 121.0, 113.0, 33.2, 21.6, 8.4. HRMS ESI (+ ve) for $C_{18}H_{18}NO_3S$ [M + H^+]: calcd 328.1001, found 328.1000, $C_{18}H_{17}NNaO_3S$ [M + Na^+]: calcd 350.0821, found 350.0809.

2.4 Cell lines

The A549, MCF7 and PC-3 cell lines were obtained from the Federal University of Rio de Janeiro. The cells line was incubated at 37 ºC in a 5% CO_2 atmosphere and cultured in Dulbecco's modified Eagle's medium (DMEM) supplemented with 10% fetal bovine serum and 1% antibiotic (10,000 U/mL penicillin; 10,000 mg/mL streptomycin).

2.5 Biological assay

2.5.1 Cytotoxicity assay

The viability of the A549, MCF7 and PC-3 cell lines was determined using sulforhodamine B (SRB) following a protocol adapted from Vichai and Kirtikara (2006). The cell lines were seeded in 96-well plates (1 × 10 cells/well) in 0.2 mL of DMEM. After 24 h, the cells were treated with a range of concentrations from 0.78 to 25 µM of 1-(1-tosyl-1*H*-indol-3-yl)propan-1-one for 72 h. Dimethylsulfoxide (0.02%) and doxorubicin hydrochloride (1.4 µM) were used as vehicle and a positive death control, respectively. After 72 h, the cells were fixed with trichloroacetic acid (30%) at 4 ºC for 1h, washed and dried at room temperature. A volume of 100 mL of the 0.057% (w/v) SRB solution was dissolved in acetic acid (1%) and added 100 µL to the wells for 30 min at room temperature. The plate was washed with acetic acid (1%) to remove excess dye and left to dry. Tris base (10 mM; pH 10.5) was used to dissolve the SRB for 30 min. Absorbances was read by spectrophotometry on a microplate reader (Synergy H1, Biotek, VT, USA) at a wavelength of 510 nm. The absorbances measured values were converted to percentage of inhibition cell growth using the following formula:

% growth inhibition = {100 - [(Abs (treated cells)/Abs. (vehicle control)) × 100]}.

The indole derivative 1-(1-tosyl-1*H*-indol-3-yl)propan-1-one had the lowest IC_{50} (concentration capable of inhibiting 50% of cell growth) against A549 cells. Therefore, considering the impact of the lung cancer, this cell line was selected to evaluate the activity of the 1-(1-tosyl-1*H*-indol-3-yl)propan-1-one on tumor cell proliferation, migration, morphology and death mechanism.

2.5.2 Hemolytic assay

The hemolytic activity of compound 1-(1-tosyl-1*H*-indol-3-yl)propan-1-one was determined according to a protocol adapted from Pita et al. (2012). The evaluation of the hemolytic activity of compound 1-(1-tosyl-1*H*-indol-3-yl)propan-1-one was carried out on human erythrocytes obtained from healthy volunteers. The study was conducted in accordance with the Declaration of Helsinki, followed the guidelines and regulations of Resolution 196/96 of the National Health Council, and was approved by the Research Ethics Committee of the Federal University of Sergipe (UFS) - University Hospital, Aracaju, Sergipe, Brazil (CEPA

55240821.7.0000.5546). A solution of erythrocytes 2% was seeded in 96-well plates and exposed a range of concentration from 32.5 to 260 μM of the compound 1-(1-tosyl-1*H*-indol-3-yl)propan-1-one. Dimethylsulfoxide (0.02%) and Triton X100 (0.1%) were used as vehicle control and positive hemolysis controls, respectively. The erythrocytes were kept under agitation at 37 ºC for 1 h. After this, the plate was centrifuged (405 xg for 5 min), and 0.15 mL of supernatant from each treatment and controls were carefully removed and transferred to another plate. Hemoglobin quantification was assessed using the absorbance of the supernatant in a spectrophotometer at a wavelength of 510 nm (Synergy H1, Biotek, VT, USA).

2.5.3 Clonogenic assay

The clonogenic assay was performed following a protocol adapted from Franken et al. (2006). A549 cells were seeded in a 6-well plate (3×10^2 cells/well) in 2 mL of DMEM. After 24 h, the cells were exposed to 1.3, 2.6 or 5.2 μM of 1-(1-tosyl-1*H*-indol-3-yl)propan-1-one for 72 h. Dimethylsulfoxide (0.02%) and doxorubicin hydrochloride (1.4 μM) were used as a vehicle control and a positive death control, respectively. After this time, the medium containing treatments were discarded, and treatment-free DMEM was added to the wells and the plate was left in appropriate culture condition for five additional days. Then, the cells were fixed with a solution of methanol and acetic acid (3:1) for 5 min and stained with 0.5% crystal violet in water for 30 min. Finally, after washing and drying the wells were photographed, and colony formation was analyzed using ImageJ software.

2.5.4 Wound healing assay

The potential of compound 1-(1-tosyl-1*H*-indol-3-yl)propan-1-one to inhibit A549 cell migration was assessed following a protocol adapted from Rodriguez et al. (2005). A549 cells were seeded in 12-well plate (3×10^5 cells/well) in 1 mL of DMEM. After 24 h, a stripe was made down the center of each well with a p200 yellow tip to remove cells from this area and the loose cells were removed by washing. The cells were then exposed to 1.3, 2.6, or 5.2 μM of 1-(1-tosyl-1*H*-indol-3-yl)propan-1-one for 48 h. Dimethylsulfoxide (0.02%) and doxorubicin hydrochloride (1.4 μM) were used as vehicle control and positive death control, respectively. The wound area was photographed at 0, 24 and 48 h under an inverted optical microscope (Olympus, IX81) to observe the wound closure.

2.5.5 Cell morphology assay

Analysis of cell morphology by fluorescence microscopy was carried out according to a protocol adapted from Wallberg et al. (2016). The A549 cells were seeded in a 24-well plate (2 × 10 cells/well) in 0.5 mL of DMEM. After 24 h, the cells were exposed to 1.3, 2.6, or 5.2 μM 1-(1-tosyl-1*H*-indol-3-yl)propan-1-one for 24 h. Dimethylsulfoxide (0.02%) and doxorubicin hydrochloride (1.4 μM) were used as a vehicle control and a positive death control, respectively. After treatment, the cells were fixed with formaldehyde (4%) and permeabilized with Triton X-100 (0.2%). The F-actin filaments in cytoskeleton of the cells was stained with phalloidin conjugated to the fluorochrome FITC, and the cell nucleus was counterstained with DAPI. Photographs were taken using a fluorescence microscope (Olympus IX81).

2.5.6 Cell death evaluation by flow cytometry

Analysis of cell death by Annexin V/PI flow cytometry was performed following a protocol from Rieger et al. (2011). A549 cells were seeded in a 12-well plate (2×10^5 cells/well) in 1 mL DMEM. After 24 h, the cells were exposed to 1.3, 2.6, or 5.2 μM 1-(1-tosyl-1*H*-indol-3-yl)propan-1-one for 24 h. Dimethylsulfoxide (0.02%) and doxorubicin hydrochloride (1.4 μM) were used as a vehicle control and a positive death control, respectively. After treatment, the cells were dissociated with trypsin/EDTA solution (1X), transferred to 2 mL microtubes and centrifuged. After washing, the cells were resuspended in Annexin binding buffer 1X and stained using Dead Cell Apoptosis Kit following the manufacturer's recommendations. The samples (30,000 cells) were analyzed on a flow cytometer (Invitrogen™ Attune™ NxT Flow Cytometer). According to staining cells were considered: viable (Annexin V $FITC^-/PI^-$), early apoptosis (Annexin V $FITC^+/PI^-$), late apoptosis (Annexin V $FITC^+/PI^+$) and necrosis (Annexin V $FITC^-/PI^+$) (Rieger et al., 2011).

2.6 Statistical analysis

The tests were carried in three independent experiments, and the results are presented as the means and 95% confidence intervals. Analyses and graphs, as well as the IC_{50}, were obtained using GraphPad Prism™ software version 9.0 (GraphPad Software, USA). The ImageJ™ software was used to analyze the images. ANOVA followed by Dunnett's post-test was used for comparisons between groups. Values of $p < 0.05$ were considered to indicate statistical significance.

3 RESULTS

3.1 Synthesis

1-(1-Tosyl-1*H*-indol-3-yl)propan-1-one was synthesized via a two-step process starting with indole, comprising a tosylation reaction using TsCl, TEBA, and NaOH in DCM, followed by a regioselective Friedel-Crafts reaction using propionyl chloride and $AlCl_3$ in anhydrous DCM, as depicted in Scheme 1.

The structure of target compound **3** was elucidated using mp, IR, ^{1}H-NMR, ^{13}C-NMR, and high-resolution mass spectroscopic methods. Synthesized compound was obtained in 74% yield after recrystallization from 10% EtOAc in hexanes and its spectral data is in full agreement with the proposed structure. The IR spectrum shows a strong stretching C = O band at 1662. ^{1}H NMR spectrum shows a typical $COCH_2$ quartet at 2.95 ppm and two CH_3 peaks, one triplet at 1.26 ppm and one singlet at 2.37. The ^{13}C spectrum shows a C = O peak at 196.8 ppm, two CH_3 peaks at 8.4 and 21.6 ppm in addition to a CH_2 peak at 33.2 ppm. The resonances of aromatic protons and carbons were observed at their predicted chemical shifts. High resolution mass spectra show the molecular ion peak $[M + H^+]$ at 328.1000, corroborating with the calculated value (328.1001).

3.2 Indole derivative 1-(1-tosyl-1*H*-indol-3-yl)propan-1-one inhibits cell growth of tumor cell lines

In this study, the cytotoxicity of the compound 1-(1-tosyl-1*H*-indol-3-yl)propan-1-one was performed in A549, MCF7 and PC-3 cell lines. The classification proposed by Mahmoud et al. (2011) was used to categorize the cell growth inhibition (GI) by the compound into three levels: low activity (GI < 50%), moderate activity (GI 51–75%), and high activity (GI > 75%). 1-(1-tosyl-1*H*-indol-3-yl)propan-1-one shows high inhibitory activity in A549 and PC3 cell lines at a concentration of 25 μM. Furthermore, moderate activity was observed in the A549 (3.12–12.5 μM), MCF7 (25 μM) and PC-3 (6.25 μM) cell lines (Fig. 1). Among the cell lines tested, the 1-(1-tosyl-1*H*-indol-3-yl)propan-1-one exhibited higher inhibition activity in the A549 cell line.

Also, IC_{50} of the 1-(1-tosyl-1*H*-indol-3-yl)propan-1-one were calculated for each tumor cell lines and presented in Table 1. In all the tumor cell lines, the IC_{50} of the compound was less than or equal to 10 μM. And, in the A549 cell line, the IC_{50} was approximately 4 times lower than in the MCF7 and 3 times lower than that in the PC-3.

Because of the relevance of lung cancer, once it has the highest mortality rate worldwide, and the low IC_{50} presented by the compound in A549 cell line, this tumor cells was selected for the other biological assays.

Table 1
IC_{50} values determined for the indole derivative 1-(1-tosyl-1*H*-indol-3-yl)propan-1-one against A549, MCF7 and PC-3.

Compound (μM)	**Cell line**		
	A549	**MCF7**	**PC-3**
1-(1-tosyl-1*H*-indol-3-yl)propan-1-one	2.6 (2.0–3.3)	10.0 (7.1–16.1)	7.8 (5.4–11.9)
Doxorubicin	1.4 (1.2–2.3)	2.8 (2.2–3.7)	5.0 (4.1–6.2)

The values are expressed as the means ± 95% confidence intervals of at least three independent experiments after 72 hours of treatment with the indole derivative 1-(1-tosyl-1*H*-indol-3-yl)propan-1-one.

The biological tests were performed at 1.3, 2.6, and 5.2 μM of the compound 1-(1-tosyl-1*H*-indol-3-yl)propan-1-one. These concentrations were defined based on the IC_{50} value and are equivalent to half and twofold the IC_{50} value. For the positive control of death, doxorubicin value at its IC_{50} (1.4 μM) was used.

3.3 Indole derivative 1-(1-tosyl-1H-indol-3-yl)propan-1-one had no hemolytic activity in human erythrocytes

The hemolytic assay was performed to evaluate the cytotoxic activity of compound 1-(1-tosyl-1*H*-indol-3-yl)propan-1-one in human erythrocytes. For this, erythrocytes were exposed of concentrations up to 100 times the IC_{50} of the compound in A549 cell line. 1-(1-tosyl-1*H*-indol-3-yl)propan-1-one had no hemolytic effect on human erythrocytes at the concentrations tested, compared with the positive control (Triton X100), that showed 100% hemolytic activity. Negative control, DMSO exhibited no hemolytic effect on human erythrocytes (Fig. 2).

3.4 Indole derivative 1-(1-tosyl-1*H*-indol-3-yl)propan-1-one inhibits colony formation of A549 cell line

According to the representative image of the clonogenic assay of the A549 cell line, the number of colonies decreased as the concentration of 1-(1-tosyl-1*H*-indol-3-yl)propan-1-one increased (Fig. 3A). In the analysis of the percentage of colonies, there was a 97% reduction at the highest concentration of 1-(1-tosyl-1*H*-indol-3-yl)propan-1-one compared to the control. Doxorubicin reduced the number of colonies of the A549 cell line by 95% (Fig. 3B).

3.5 Indole derivative 1-(1-tosyl-1H-indol-3-yl)propan-1-one inhibits migration of A549 cell line

In the representative image of migration of the A549 cell line, it was possible to observe an inhibition of wound closure at the highest concentrations (2.6 and 5.2 μM) of compound 1-(1-tosyl-1*H*-indol-3-yl)propan-1-one (Fig. 4A). According to the analysis of the percentage of wound closure, 1-(1-tosyl-1*H*-indol-3-yl)propan-1-one (5.2 μM) inhibited the migration of A549 cell line by 97% after 24 h and by 94% after 48 h. At a concentration of 2.6 μM, it inhibited cell migration by 87% after 24 h and 69% after 48 h of treatment. Additionally, at the lowest concentration of 1.3 μM compound 1-(1-tosyl-1*H*-indol-3-yl)propan-1-one inhibited cell migration by 33% after 48 h of treatment, but do not inhibit significatively wound closure after 48 h. All comparisons were made with the untreated negative control at the same time points. Compared with the untreated negative control, the doxorubicin was able to inhibit the migration of A549 cell line by 59% after 48 h of treatment (Fig. 4B).

3.6 The indole derivative 1-(1-tosyl-1H-indol-3-yl)propan-1-one induces morphological changes in A549 cell line

Analysis of the morphology of A549 cell line revealed stress bundles in the F-actin filaments, loss of cytoplasmic volume, apoptotic projections in the cytoskeleton and DNA fragmentation in the nucleus. These morphological changes were observed at all tested concentrations of compound 1-(1-tosyl-1*H*-indol-3-yl)propan-1-one. In addition, the presence of rounded cells was observed at 2.6 μM, a shape that is not present in non-treated A549 cell line. The loss of cytoplasmic volume and the presence of apoptotic projections in the cytoplasm were observed in cells treated with doxorubicin (Fig. 5).

3.6 Indole derivative 1-(1-tosyl-1H-indol-3-yl)propan-1-one induces apoptosis in A549 cell line

Figure 6. Quantitative analysis of the percentage of viable cells, early and late apoptosis and necrosis in the A549 cell line after treatment with the indole derivative 1-(1-tosyl-1*H*-indol-3-yl)propan-1-one for 24 h. **(A)** Dot plot from flow cytometry divided into four quadrants: viable cells (Annexin V-/PI-), early apoptosis (Annexin V+/PI-), late apoptosis (Annexin V+/PI+) and necrosis (Annexin V-/PI+). **(B)** Doxorubicin (10 μM)

was used as positive control and DMSO (0.02%) was used as negative control (Cnt) of death, respectively. Analyses between the treatments and control groups were carried out using ANOVA, followed by Dunnet's posttest (*) $P < 0.01$; (**) $P < 0.001$. The data represent the mean ± SD of three independent experiments.

4 DISCUSSIONS

Our findings demonstrated the cytotoxic activity of an indole derivative compound against tumor cells. In fact, the literature has already proven that indole has antiproliferative activity against HeLa, colorectal adenocarcinoma, breast, acute promyelocytic leukemia and histiocytic lymphoma cell lines, a human myeloid leukemia cell line, lymphoma and glioma (Preti et al., 2018; Danisman-Kalindemirtas et al., 2022; Andrade et al., 2024).

In our study, the synthetic indole derivative 1-(1-tosyl-1*H*-indol-3-yl)propan-1-one presented IC_{50} less than or equal to 10 uM against A549, MCF7 and PC-3 tumor cell lines. Interestingly, according to Kuete et al. (2014), for a compound to be considered a potent antitumor agent, its IC_{50} value must be less than 10 μM after 72 h of treatment. Consistent with these results, other study of our group observed that indole and its derivatives were able to inhibit the growth of the tumor cells (A549, C6 and B16F10) (Andrade et al., 2024). Synthetic derivatives could be more effective in its cytotoxicity activity than indole, as observed in Ahmad et al. (2019), in which indole derivatives were two to fivefold more cytotoxic in carcinoma cell lines pancreas (BxPC-3), prostate (LNCaP, C4-2B and PC3) and triple-negative breast carcinoma (MDA-MB-231) than indol.

Another analysis carried out in this study was the analysis of the toxicity of compound 1-(1-tosyl-1*H*-indol-3-yl)propan-1-one on human erythrocytes. The hemolysis test is used to assess the toxicity of compounds in nontumor cells (Saebo et al., 2023). The erythrocyte membrane is delicate and can undergo changes after exposure to compounds, including the possibility of rupture of the cell membrane (Evans et al., 2013). In our study, no hemolysis was observed in human erythrocytes after exposure to the evaluated compound, even at the highest concentration of 100 × IC_{50} of the compound, which was evaluated in the A549 cell line. In agreement with this study, Andrade et al. (2024) evaluated the hemolytic activity of a series of compounds derived from indol, and no hemolysis was observed in human erythrocytes. Santos et al. (2023) also reported no hemolytic activity in human erythrocytes exposed to a synthetic derivative of a natural product.

The observed cytotoxicity of the synthesized indole derivative may be attributed to the aryl group attached to the benzene ring connected to both the oxygen moiety and the carbon chain, thereby increasing molecular size and potentially reducing hydrophilic interactions. These structural modifications likely enhanced cytotoxic efficacy against tumor cells (Andrade et al., 2024; Rieger et al., 2011).

An attempt to evaluate the anti-proliferative and the anti-clonogenic effect of 1-(1-tosyl-1*H*-indol-3-yl)propan-1-one the clonogenic assay was performed. This assay consists of evaluating the proliferative viability and colony-forming capacity of a single cell after a period of incubation, in which the cells are maintained under favorable growth conditions (Franken et al., 2006). In this study, we observed that

compared with no treatment, 1-(1-tosyl-1*H*-indol-3-yl)propan-1-one inhibited the formation of colonies of the A549 cell line. Other studies have shown a reduction in the number of colonies of glioma cells (C6) after treatment with heterocyclic compounds, a group to which indol belongs (Ramirez et al., 2020; Andrade et al., 2024). Also, Sabol et al. (2000) showed that indolic phytoalexins had an antiproliferative effect on the B16 and L1210 cell lines.

Tumor cells can detach from the tumor mass and migrate to new tissues and organs. The search for new compounds that can inhibit cell migration may inhibit the invasiveness of tumor cells, contributing to a positive prognosis for patients with this disease (Motta et al., 2024). Our results showed that treatment with compound 1-(1-tosyl-1*H*-indol-3-yl)propan-1-one inhibited the migration of A549 cell. Consistent with the results of this study, Andrade et al. (2024) reported that indolic derivatives inhibited the migration of glioma cell lines. Ma et al. (2017) observed that treatment with the compound deoxyarbutin, derived from a natural product, was able to inhibit tumor metastasis *in vitro* and *in vivo* in melanoma through an apoptotic pathway associated with p38-mediated mitochondria (Ma et al., 2017). Inhibiting the formation of clones and the migration of tumor cells directly interferes with the process of metastasis, both by inhibiting the migration of these cells and their establishment in a new tissue.

The loss of cell migration ability may also be associated with functional alterations in the cytoskeleton. The cytoskeleton is made up of a network of proteins that give shape to the cell and provides structural support, allows for the mobility of intracellular organelles, which are important factors in cell movement and consequently, cell migration (Linartevichi et al., 2021).

In this study, we observed that 1-(1-tosyl-1*H*-indol-3-yl)propan-1-one induces changes in the morphology of A549 cell line. As the concentration of compound 1-(1-tosyl-1*H*-indol-3-yl)propan-1-one increased, there is a decrease in the cytoplasmic volume, reduction in the number of cells, and an increase in projections of cytoplasm. Also, in the nucleus of the cells was observed DNA fragmentation. To date, these changes show that compound 1-(1-tosyl-1*H*-indol-3-yl)propan-1-one reduces the migratory capacity and proliferation of cancer cells.

The death of tumor cells by apoptosis is less harmful because it is largely regulated. In this type of death there is no leakage of cytoplasmic or nuclear material from the cells, reducing or preventing an inflammatory process (Chen et al., 2018). Our results showed that a high percentage of the A549 cells underwent initial apoptosis after treatment with the highest concentrations of compound 1-(1-tosyl-1*H*-indol-3-yl)propan-1-one.

The evasion of cells from apoptosis is one of the factors responsible not only for tumor emergence, development and progression but also for the resistance of tumor cells to current therapies (Pistrito et al., 2016). Identifying bioactive compounds that can stimulate tumor cell death via apoptosis is extremely important for cancer treatment. Most of the anticancer drugs currently being tested precisely exploit apoptosis signaling pathways as a way of seeking drugs with less toxic effects on non-tumor cells (Pistrito et al., 2016; Newton et al., 2024).

Annexin V/FITC binds to apoptotic cells by interacting with phosphatidylserine externalized on the membrane of cells undergoing apoptosis. On the other hand, PI is an indicator of necrotic cells, as it binds to the DNA of cells with altered membrane integrity (Galhardas, 2014) (LAKSHMANAN; BATRA, 2013). Studies in the literature observed an increase in annexin binding in glioma, lung cancer and melanoma cells after treatment with synthetic derivatives of natural products, indicating that the mechanism of cell death in these cells was apoptosis (Andrade et al., 2024; dos Santos et al., 2023; de Franca et al., 2021). Preti and collaborators (2018) analyzed the antiproliferative activity of indole-based chalcones against the HeLa, HT29, MCF-7 and U-937 cell lines. In these compounds, one of the aryl rings was replaced by an indole. The authors suggest that this modification caused an overexpression of Bcl-2 (U-937/Bcl-2) observed via cell cycle arrest in the G2 and M phases, and induced apoptosis in these cell lines.

This study demonstrates the potential of 1-(1-tosyl-1*H*-indol-3-yl)propan-1-one to inhibit proliferation of tumor cells. In addition, to not having a toxic effect on human erythrocytes. Also, the results of the inhibition of colony formation, the inhibition of migration and the analysis of cell death mechanisms, show that the evaluated compound has cytotoxic effects on tumor cells and no toxic effects on healthy cells. Further studies on the mechanism of action of the proposed compound are needed to fully characterize and analyze its antitumor potential *in vitro* and *in vivo*.

Abbreviations

A549 Human Lung Carcinoma Epithelial cell line

ANOVA Analysis of variance

DAPI 4',6-Diamidine-2-Phenylindole Dihydrochloride

DMEM Dulbecco's Modified Eagle Medium

DMSO Dimethylsulfoxide

DOX Doxorubicin

EDTA Ethylenediamine tetra acetic acid

FITC Fluorescein Isothiocyanate (Fluorescein isothiocyanate)

IC_{50} Inhibition Concentration for 50% of cells

MCF7 Human Breast Adenocarcinoma Epithelial cell line

PBS Phosphate Buffer Saline (Phosphate buffered saline)

PC-3 Human Prostate Adenocarcinoma Epithelial cell line

PI Propidium Iodide (Propridium Iodide)

SFB Fetal bovine sérum

Declarations

Ethics approval and consent to participate

This study with human erythrocytes was carried out in accordance with the Declaration of Helsinki, following the guidelines and norms of Resolution 196/96 of the National Health Council, and was approved by the Research Ethics Committee of the Federal University of Sergipe (UFS) - University Hospital, Aracaju, Sergipe, Brazil (CEPA 55240821.7.0000.5546).

Consent for publication

Not applicable

Competing interests

The authors declare that they have no competing interests.

Funding

This work was carried out with the support and scholarships of CNPq, National Council for Scientific and Technological Development – Brazil, grant # 402755/2016-2.

Author Contribution

JB analyzed the experiments and were the major contributors in writing the manuscript, performed all the experiments with the authors, synthesized the analyzed molecule. CC supervision, analyzed the experiments and were the major contributors in writing the manuscript. MF analyzed the experiments and were the major contributors in writing the manuscript. SC synthesized the analyzed molecule, participated of writing of manuscript. MM, JS and CO participated of the execution of the experiments. RA participated of writing of manuscript. All authors commented and approved the final version.

Acknowledgements

Not applicable

Availability of data and materials

The datasets used and/or analysed during the current study available from the corresponding author on reasonable request.

References

1. AHMAD, A. et al. Pentafluorophenyl Substitution of Natural Di(indol-3-yl) methane Strongly Enhances Growth Inhibition and Apoptosis Induction in Various Cancer Cell Lines. **Chemistry & Biodiversity**, v. 16, n. 4, 19 abr. 2019.
2. ANDRADE, A. K. DE S. et al. Anti-migratory and cytotoxic effect of indole derivative in C6 glioma cells. **Toxicology in Vitro**, v. 96, p. 105786, abr. 2024.
3. ASMA, S. T. et al. Natural Products/Bioactive Compounds as a Source of Anticancer Drugs. **Cancers**, v. 14, n. 24, p. 6203, 15 dez. 2022a.
4. ASMA, S. T. et al. Natural Products/Bioactive Compounds as a Source of Anticancer Drugs. **Cancers**, v. 14, n. 24, 15 dez. 2022b.
5. CARVALHO, H. D. A. Radioterapia no câncer de pulmão. **Jornal de Pneumologia**, v. 28, n. 6, p. 345–350, nov. 2002.
6. CHEN, Q.; KANG, J.; FU, C. The independence of and associations among apoptosis, autophagy, and necrosis. **Signal Transduction and Targeted Therapy**, v. 3, n. 1, p. 18, 1 jul. 2018.
7. DADASHPOUR, S.; EMAMI, S. Indole in the target-based design of anticancer agents: A versatile scaffold with diverse mechanisms. **European Journal of Medicinal Chemistry**, v. 150, p. 9–29, abr. 2018.
8. DANIŞMAN-KALINDEMIRTAŞ, F. et al. Selective Cytotoxic Effects of 5-Trifluoromethoxy-1H-indole-2,3-dione 3-Thiosemicarbazone Derivatives on Lymphoid-originated Cells. **Anti-Cancer Agents in Medicinal Chemistry**, v. 22, n. 2, p. 349–355, jan. 2022.
9. DE FRANCA, M. N. F. et al. Anti-proliferative and pro-apoptotic activity of glycosidic derivatives of lawsone in melanoma cancer cell. **BMC Cancer**, v. 21, n. 1, p. 662, 2 dez. 2021.
10. DENISENKO, T. V.; BUDKEVICH, I. N.; ZHIVOTOVSKY, B. Cell death-based treatment of lung adenocarcinoma. **Cell Death & Disease**, v. 9, n. 2, p. 117, 25 jan. 2018.
11. DOS SANTOS, E. W. P. et al. Inhibitory effect of O-propargyllawsone in A549 lung adenocarcinoma cells. **BMC Complementary Medicine and Therapies**, v. 23, n. 1, p. 333, 20 set. 2023.
12. ESCAMILLA-RAMÍREZ, A. et al. Autophagy as a Potential Therapy for Malignant Glioma. **Pharmaceuticals**, v. 13, n. 7, p. 156, 19 jul. 2020.
13. EVANS, B. C. et al. Red Blood Cell Hemolysis Assay for the Evaluation of pH-responsive Endosomolytic Agents for Cytosolic Delivery of Biomacromolecular Drugs. **Journal of Visualized Experiments**, n. 73, 9 mar. 2013.
14. FARONI, L. et al. Role of Stereotactic Radiation Therapy in Operable and Inoperable Early-Stage Non-small Cell Lung Cancer. **Current Treatment Options in Oncology**, v. 23, n. 9, p. 1185–1200, 15 set. 2022.

15. FRANKEN, N. A. P. et al. Clonogenic assay of cells in vitro. **Nature Protocols**, v. 1, n. 5, p. 2315–2319, 21 dez. 2006.
16. GUERRA, R. L. et al. Cost Utility of Target Therapies Compared to Dacarbazine for First-Line Treatment of Advanced Non-Surgical and Metastatic Melanoma in the Brazilian National Health System. **Value in Health Regional Issues**, v. 20, p. 103–109, dez. 2019.
17. GUERRERO-BELTRÁN, C. E. et al. Protective effect of sulforaphane against oxidative stress: Recent advances. **Experimental and Toxicologic Pathology**, v. 64, n. 5, p. 503–508, jul. 2012.
18. HECHT, S. S. INHIBITION OF CARCINOGENESIS BY ISOTHIOCYANATES*. **Drug Metabolism Reviews**, v. 32, n. 3–4, p. 395–411, 10 jan. 2000.
19. HUTCHINSON, B. D. et al. Spectrum of Lung Adenocarcinoma. **Seminars in Ultrasound, CT and MRI**, v. 40, n. 3, p. 255–264, jun. 2019.
20. INSTITUTO NACIONAL DE CÂNCER JOSÉ ALENCAR GOMES DA SILVA (INCA). Disponível em: <INCA - Instituto Nacional de Câncer |>.
21. INSTITUTO NACIONAL DE CÂNCER JOSÉ ALENCAR GOMES DA SILVA (INCA). **Ambiente, trabalho e câncer: aspectos epidemiológicos, toxicológicos e regulatórios**. Rio de Janeiro, 150 2021a. Disponível em: https://www.inca.gov.br/sites/ufu.sti.inca.local/files/media/document/ambiente_trabalho_e_cancer_-_aspectos_epidemiologicos_toxicologicos_e_ regulatorios.pdf.
22. INSTITUTO NACIONAL DE CÂNCER JOSÉ ALENCAR GOMES DA SILVA (INCA). **Detecção precoce do câncer**. Rio de Janeiro, 2021b. Disponível em: https://www.inca.gov.br/publicacoes/ livros/deteccao-precoce-do-cancer.
23. KELLY, P. M. et al. Synthesis, antiproliferative and pro-apoptotic activity of 2-phenylindoles. **Bioorganic & Medicinal Chemistry**, v. 24, n. 18, p. 4075–4099, set. 2016.
24. KUETE, V. et al. Cytotoxicity of four Aframomum species (A. arundinaceum, A. alboviolaceum, A. kayserianum and A. polyanthum) towards multi-factorial drug resistant cancer cell lines. **BMC Complementary and Alternative Medicine**, v. 14, n. 1, p. 340, 19 dez. 2014.
25. LINARTEVICHI, V. F. et al. Patogenia das doenças relacionadas ao citoesqueleto: uma revisão da literatura/ Pathogenics of cytoskeleton-related diseases: a review. **Brazilian Journal of Development**, v. 7, n. 6, p. 60578–60593, 18 jun. 2021.
26. MA, L. et al. Deoxyarbutin displays antitumour activity against melanoma in vitro and in vivo through a p38-mediated mitochondria associated apoptotic pathway. **Scientific Reports**, v. 7, n. 1, p. 7197, 3 ago. 2017.
27. MAHMOUD, T. S. et al. In vitro cytotoxic activity of Brazilian Middle West plant extracts. **Revista Brasileira de Farmacognosia**, v. 21, n. 3, p. 456–464, jun. 2011.
28. MONTALVÃO, M. M. et al. Cytotoxic activity of essential oil from Leaves of Myrcia splendens against A549 Lung Cancer cells. **BMC Complementary Medicine and Therapies**, v. 23, n. 1, p. 139, 2 maio 2023.

29. MOTTA, J. M. et al. A low-anticoagulant heparin suppresses metastatic dissemination through the inhibition of tumor cell-platelets association. **Biomedicine & Pharmacotherapy**, v. 171, p. 116108, fev. 2024.
30. NEWMAN, D. J.; CRAGG, G. M. Natural Products as Sources of New Drugs over the Nearly Four Decades from 01/1981 to 09/2019. **Journal of Natural Products**, v. 83, n. 3, p. 770–803, 27 mar. 2020.
31. NEWTON, K. et al. Cell death. **Cell**, v. 187, n. 2, p. 235–256, jan. 2024.
32. OBENG, E. Apoptosis (programmed cell death) and its signals - A review. **Brazilian Journal of Biology**, v. 81, n. 4, p. 1133–1143, dez. 2021.
33. OROUJI, N. et al. Glucosinolates in cancer prevention and treatment: experimental and clinical evidence. **Medical Oncology**, v. 40, n. 12, p. 344, 3 nov. 2023.
34. PÊGO-FERNANDES, P. M. et al. The role of the surgeon in treating patients with lung cancer. An updating article. **Sao Paulo Medical Journal**, v. 139, n. 3, p. 293–300, jun. 2021.
35. PISTRITTO, G. et al. Apoptosis as anticancer mechanism: function and dysfunction of its modulators and targeted therapeutic strategies. **Aging**, v. 8, n. 4, p. 603–619, 27 mar. 2016.
36. PITA, J. C. L. R. et al. In Vitro and in Vivo Antitumor Effect of Trachylobane-360, a Diterpene from Xylopia langsdorffiana. **Molecules**, v. 17, n. 8, p. 9573–9589, 10 ago. 2012.
37. PRETI, D. et al. Design, synthesis, *in vitro* antiproliferative activity and apoptosis-inducing studies of 1-(3',4',5'-trimethoxyphenyl)-3-(2'-alkoxycarbonylindolyl)-2-propen-1-one derivatives obtained by a molecular hybridisation approach. **Journal of Enzyme Inhibition and Medicinal Chemistry**, v. 33, n. 1, p. 1225–1238, 1 jan. 2018.
38. RIEGER, A. M. et al. Modified Annexin V/Propidium Iodide Apoptosis Assay For Accurate Assessment of Cell Death. **Journal of Visualized Experiments**, n. 50, 24 abr. 2011.
39. RODRIGUEZ, L. G.; WU, X.; GUAN, J.-L. Wound-Healing Assay. Em: **Cell Migration**. New Jersey: Humana Press, [s.d.]. p. 023–030.
40. SABOL, M. et al. Cytotoxic effect of cruciferous phytoalexins against murine L1210 leukemia and B16 melanoma. **Biologia 2000**, 55, 701–707 ISSN/ISBN: 0006-3088.
41. SÆBØ, I. P. et al. Optimization of the Hemolysis Assay for the Assessment of Cytotoxicity. International journal of molecular sciences, v. 24, n. 3, 2 fev. 2023.
42. SHAPIRO, T. A. et al. Human metabolism and excretion of cancer chemoprotective glucosinolates and isothiocyanates of cruciferous vegetables. **Cancer epidemiology, biomarkers & prevention: a publication of the American Association for Cancer Research, cosponsored by the American Society of Preventive Oncology**, v. 7, n. 12, p. 1091–100, dez. 1998.
43. SILVA, L. V. B. et al. Efeitos adversos e qualidade de vida em pacientes que fazem quimioterapia e radioterapia / Adverse effects and quality of life in patients under chemotherapy and radiotherapy. **Brazilian Journal of Development**, v. 8, n. 4, p. 32544–32549, 29 abr. 2022.
44. SINGH, T. P.; SINGH, O. M. Recent Progress in Biological Activities of Indole and Indole Alkaloids. **Mini-Reviews in Medicinal Chemistry**, v. 18, n. 1, 8 dez. 2017.

45. SOUNDARARAJAN, P.; KIM, J. S. Anti-Carcinogenic Glucosinolates in Cruciferous Vegetables and Their Antagonistic Effects on Prevention of Cancers. **Molecules**, v. 23, n. 11, p. 2983, 15 nov. 2018.
46. THE INTERNATIONAL AGENCY FOR RESEARCH ON CANCER (IARC). **Global Cancer Observatory**. Disponível em: <https://gco.iarc.fr/en>.
47. VICHAI, V.; KIRTIKARA, K. Sulforhodamine B colorimetric assay for cytotoxicity screening. **Nature Protocols**, v. 1, n. 3, p. 1112–1116, 17 ago. 2006.
48. WALLBERG, F.; TENEV, T.; MEIER, P. Analysis of Apoptosis and Necroptosis by Fluorescence-Activated Cell Sorting. **Cold Spring Harbor Protocols**, v. 2016, n. 4, p. pdb.prot087387, 1 abr. 2016.
49. YELDAG, G.; RICE, A.; DEL RÍO HERNÁNDEZ, A. Chemoresistance and the Self-Maintaining Tumor Microenvironment. **Cancers**, v. 10, n. 12, p. 471, 28 nov. 2018.
50. ZARBIN, A. J. G. 36ª Reunião Anual da SBQ. **Química Nova**, v. 36, n. 5, p. 621–621, 2013.

Scheme 1

Scheme 1 is available in the Supplementary Files section.

Figures

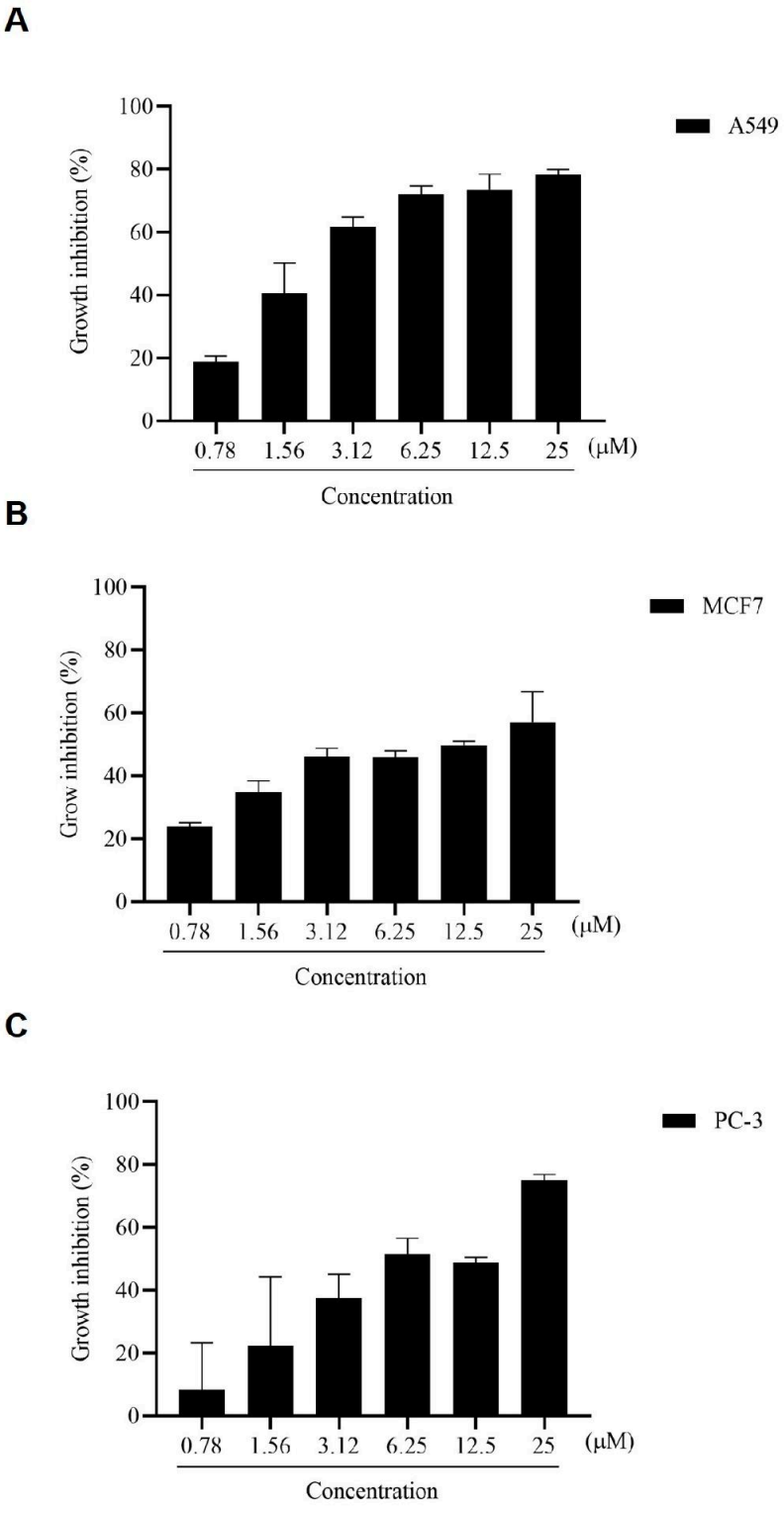

Figure 1

Percentage of growth inhibition of the A549 **(A)**, MCF7 **(B)** and PC-3 **(C)** cell lines by 1-(1-tosyl-1*H*-indol-3-yl)propan-1-one compound after 72 h. The data represent the mean ± SD of three independent experiments.

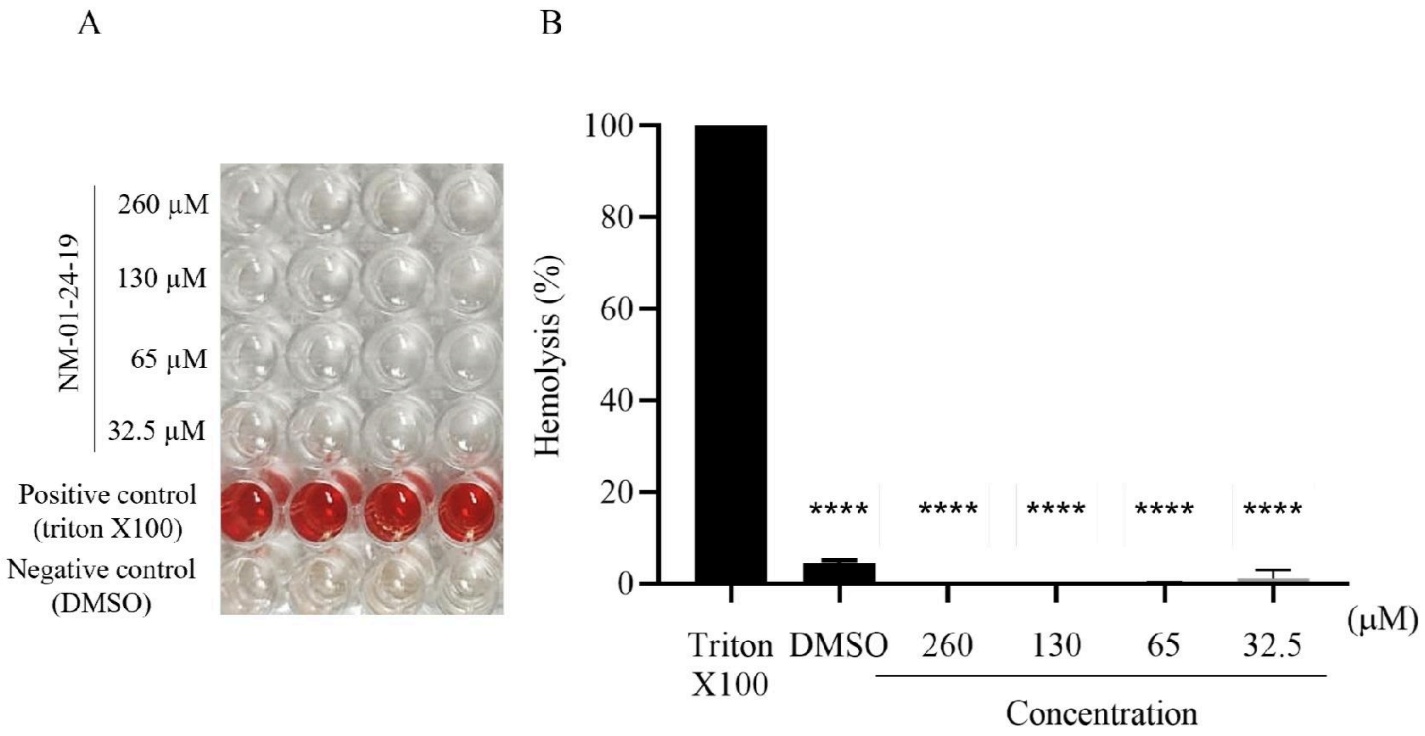

Figure 2

Hemolysis assay on human erythrocytes. **(A)** Image of wells in a representative experiment. Triton X100 (1%) was used as positive control of hemolysis and DMSO was used as vehicle control, respectively. **(B)** Graph of the percentage of hemolysis of human erythrocytes. Analyses between groups were carried out using ANOVA, followed by Dunnet's posttest (****) $p<0.0001$ compared to the control. The data represent the mean ± SD of three independent experiments carried out in quadruplicate.

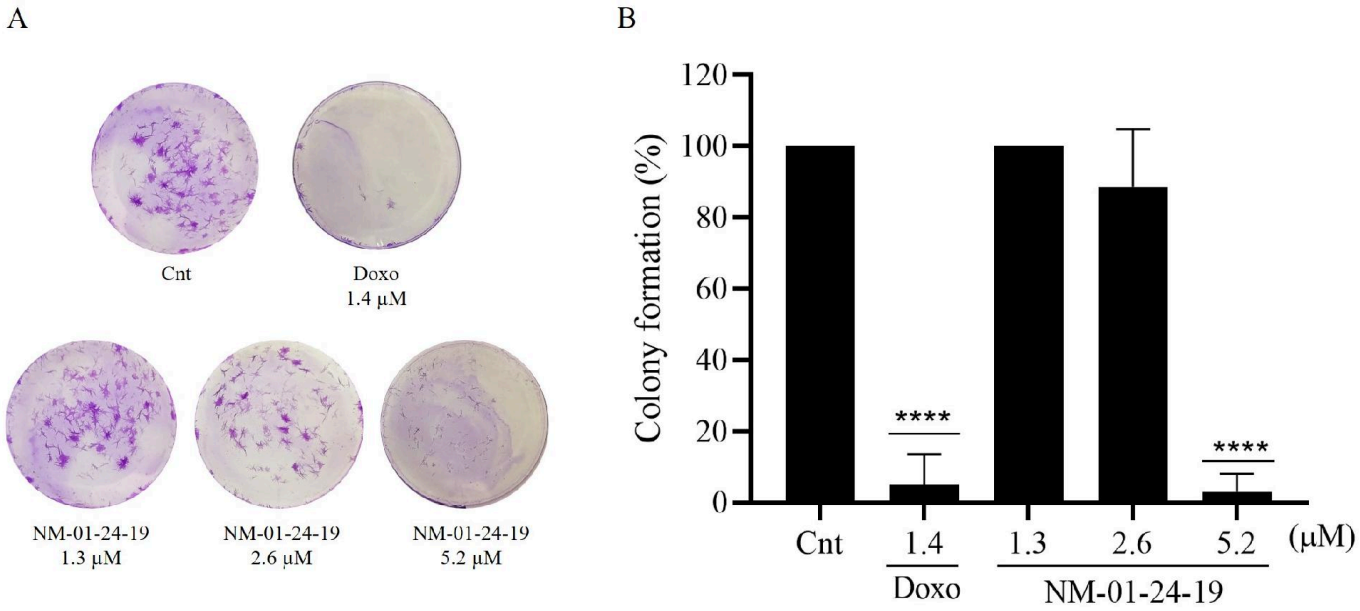

Figure 3

Inhibitory effect of the indole derivative 1-(1-tosyl-1*H*-indol-3-yl)propan-1-one on colony formation in A549 cell line. **(A)** Representative image of colony formation after 72 h of treatment and 10 days of cell growth. DMSO (0.02%) (Cnt) and doxorubicin (doxo) (1.4 μM) were used as a vehicle control and a positive death control, respectively. **(B)**Analysis of the percentage of colony formation. The differences between treatments and control were analyzed using ANOVA, followed by Dunnett's posttest (****); p<0.0001.

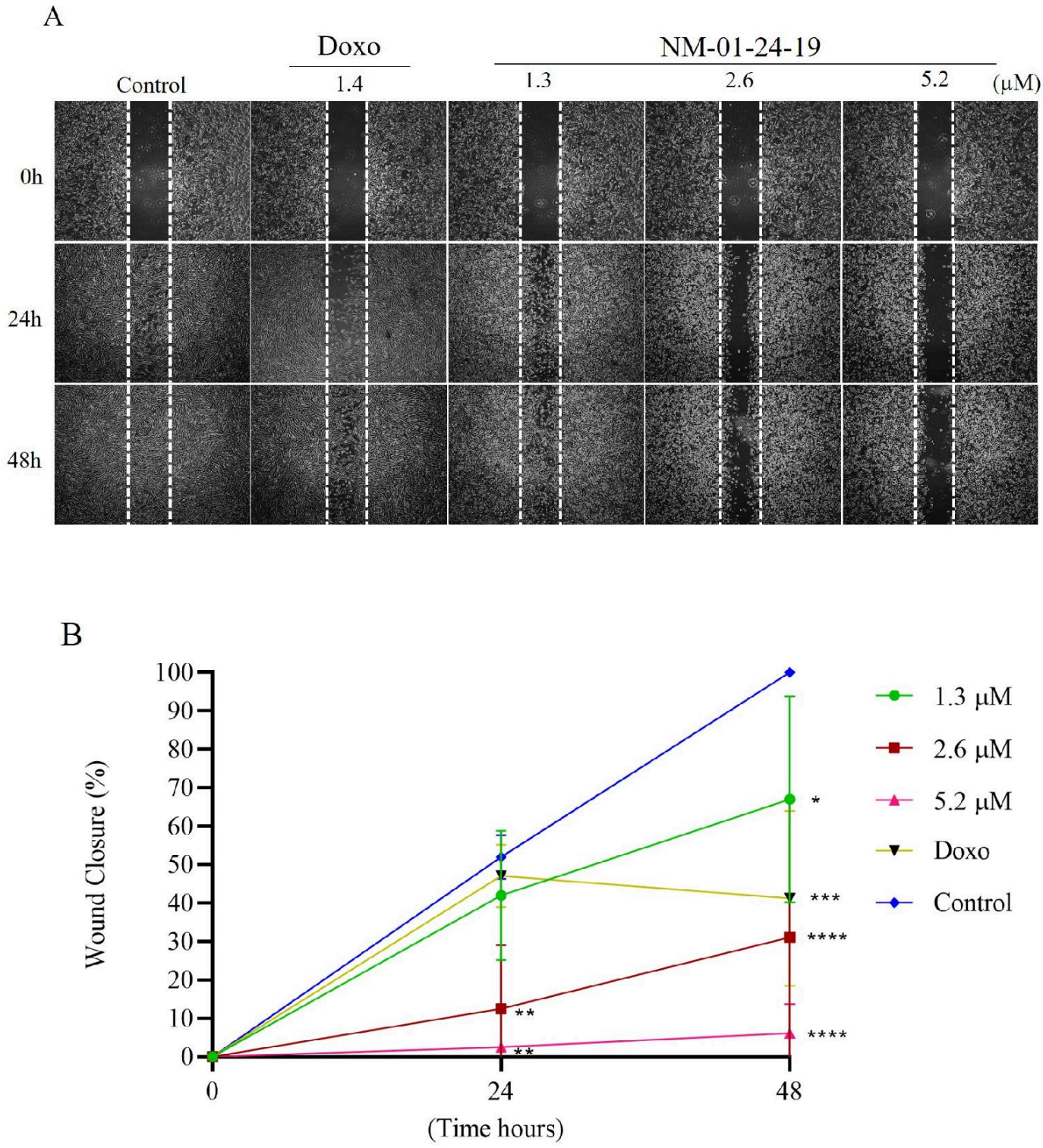

Figure 4

Inhibitory effect of the indole derivative 1-(1-tosyl-1*H*-indol-3-yl)propan-1-one on cell migration of A549 cell line. **(A)** Representative image of cell migration after 48 h of treatment. DMSO (Control) (0.02%) and doxorubicin (Doxo) (1.4 μM) were used as vehicle control and positive death control, respectively. **(B)** Analysis of the percentage of wound closure. The data represents the mean ± SD of three independent experiments. The difference between treatments and control were analyzed using Two-way ANOVA, followed by Dunnett's posttest; (*) P<0.05; (**) P<0.01; (***) P<0.001 and (****) P<0.0001. Comparisons were made between times 24 and 48 h with time 0 of each treatment.

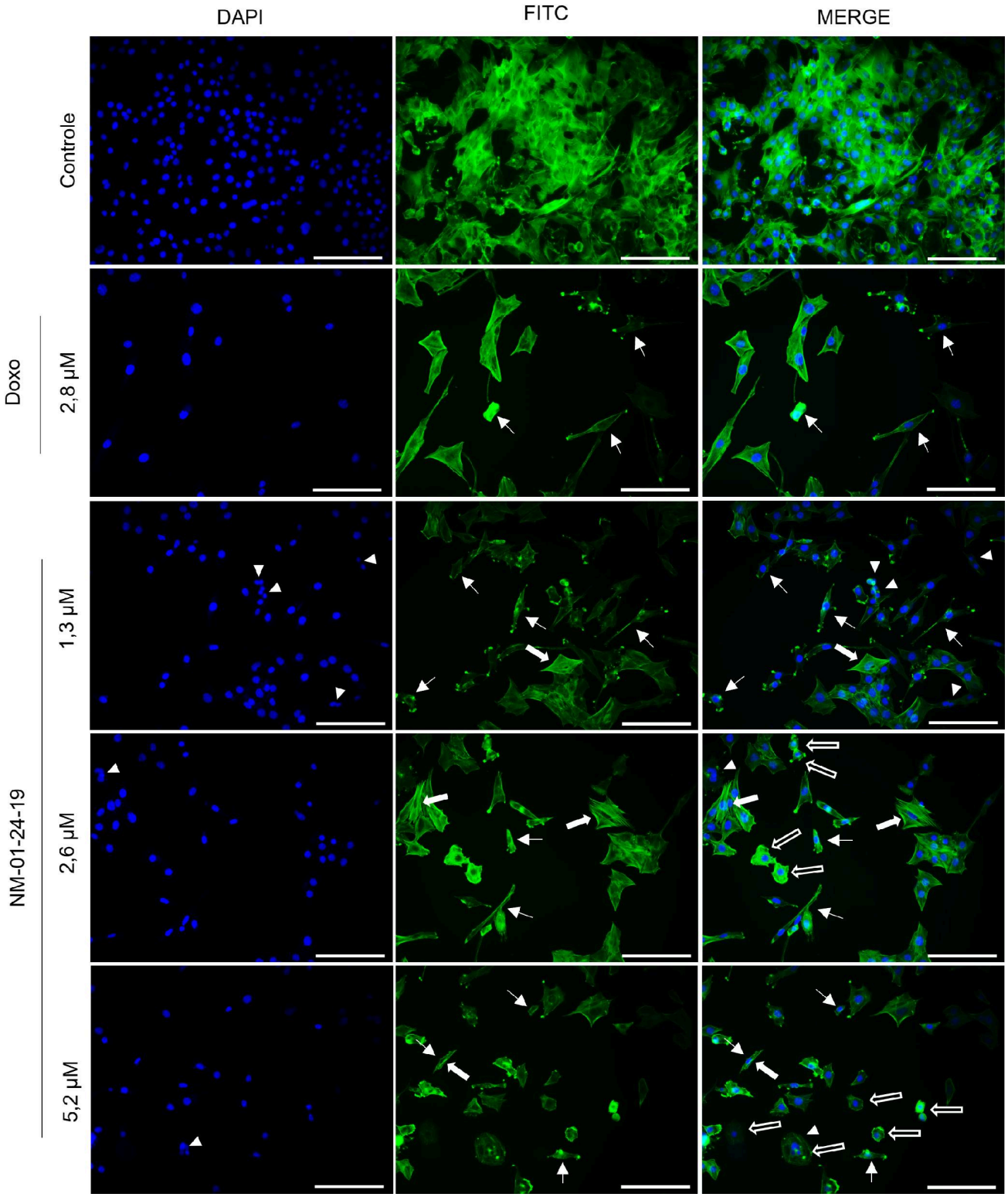

Figure 5

Morphological changes in A549 cell line after treatment with the indole derivative 1-(1-tosyl-1*H*-indol-3-yl)propan-1-one for 24 h. DMSO (Control) (0.02%) and doxorubicin (Doxo) (1.4 µM) were used as a vehicle control and a positive death control, respectively. Filled arrows indicate stress of F-actin filaments; thin arrows indicate loss of cytoplasmic volume; arrow heads indicate DNA fragmentation and hollow arrows indicate cell rounding. Bar: 100 µm.

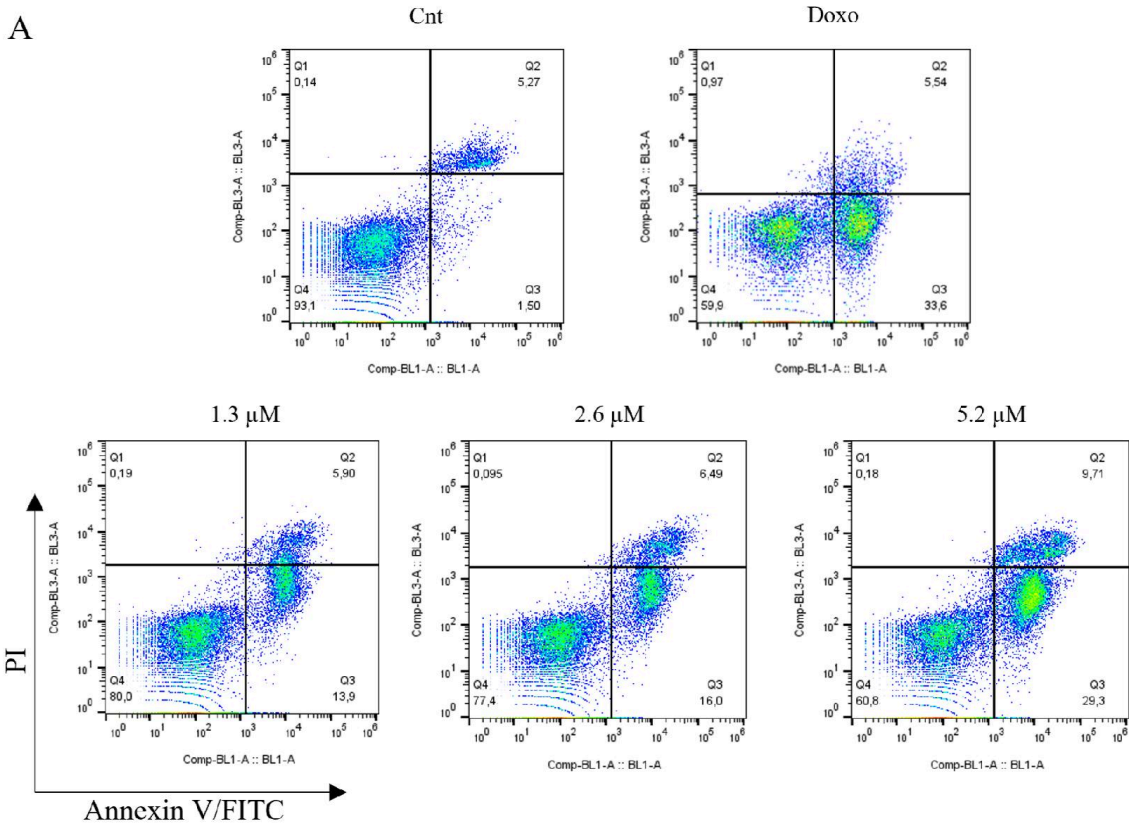

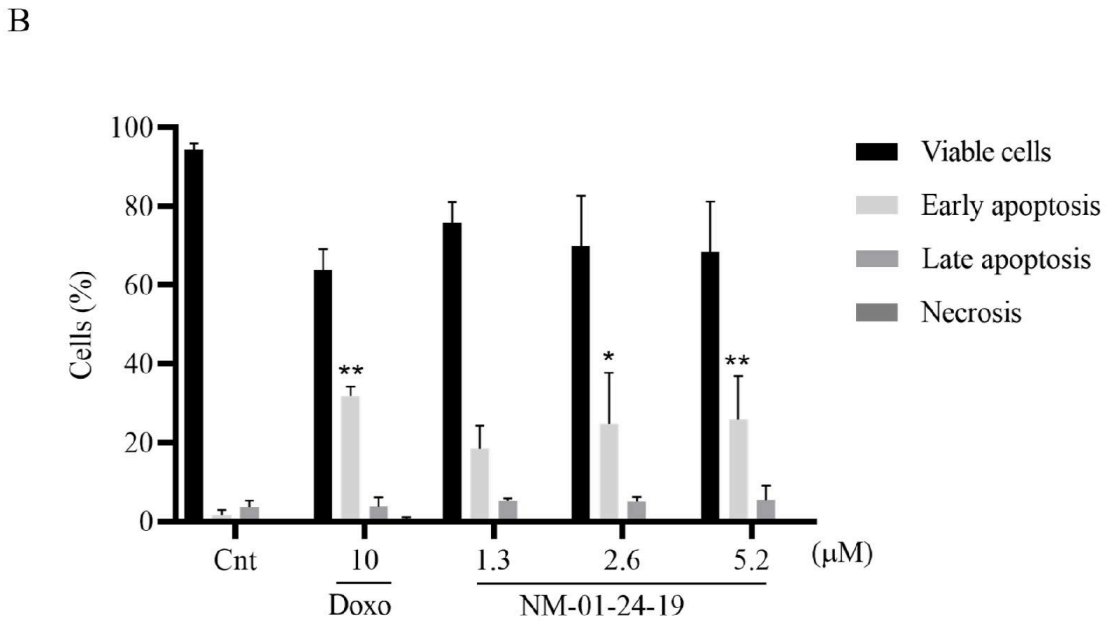

Figure 6

Quantitative analysis of the percentage of viable cells, early and late apoptosis and necrosis in the A549 cell line after treatment with the indole derivative 1-(1-tosyl-1*H*-indol-3-yl)propan-1-one for 24 h. **(A)** Dot plot from flow cytometry divided into four quadrants: viable cells (Annexin V-/PI-), early apoptosis (Annexin V+/PI-), late apoptosis (Annexin V+/PI+) and necrosis (Annexin V-/PI+). **(B)** Doxorubicin (10 µM) was used as positive control and DMSO (0.02%) was used as negative control (Cnt) of death, respectively. Analyses between the treatments and control groups were carried out using ANOVA, followed by Dunnet's posttest (*) P<0.01; (**) P<0.001. The data represent the mean ± SD of three independent experiments.

Supplementary Files

This is a list of supplementary files associated with this preprint. Click to download.

- Scheme1.jpg